ACS NANO
Cite This: ACS Nano XXXX, XXX, XXX–XXX
www.acsnano.org

ARTICLE

Unraveling Sunlight by Transparent Organic Semiconductors toward Photovoltaic and Photosynthesis

Yuqiang Liu,[†,‡] Pei Cheng,[*,†] Tengfei Li,[∥] Rui Wang,[†] Yaowen Li,[§] Sheng-Yung Chang,[†] Yuan Zhu,[†] Hao-Wen Cheng,[†,⊥] Kung-Hwa Wei,[⊥] Xiaowei Zhan,[∥] Baoquan Sun,[*,‡] and Yang Yang[*,†]

[†]Department of Materials Science and Engineering, University of California, Los Angeles, California 90095, United States

[‡]Jiangsu Key Laboratory for Carbon-Based Functional Materials and Devices, Institute of Functional Nano & Soft Materials (FUNSOM), Joint International Research Laboratory of Carbon-Based Functional Materials and Devices and [§]Laboratory of Advanced Optoelectronic Materials, College of Chemistry, Chemical Engineering and Materials Science, Soochow University, Suzhou 215123, China

[∥]Department of Materials Science and Engineering, College of Engineering, Key Laboratory of Polymer Chemistry and Physics of Ministry of Education, Peking University, Beijing 100871, China

[⊥]Department of Materials Science and Engineering, Center for Emergent Functional Matter Science, National Chiao Tung University, Hsinchu 30050, Taiwan

Supporting Information

ABSTRACT: **Because the visible and the infrared (IR) regions take up ∼47% and ∼51% of the energy in the solar spectrum (AM 1.5G standard), respectively, utilizing the visible light for plant growth and the IR light for power generation is potentially extremely exciting. IR-absorbing organic semiconductors, with localized IR absorption and visible-light transmittance, would be promising materials for this purpose. Here, flexible transparent organic photovoltaics (TOPVs) based on IR-absorbing organic materials were proposed, which can be a simple, low-cost, and promising way to utilize the IR light for electricity generation, and the penetrated visible light will be utilized for photosynthesis in plants. A power-conversion efficiency of ∼10% with an average visible transmittance of 34% was achieved for TOPV devices. Meanwhile, the side-by-side comparison showed that plants grown under the TOPVs filtered light, and those under normal sunlight yielded very similar results. These outcomes demonstrated the results from TOPV devices beyond simple photovoltaic applications.**

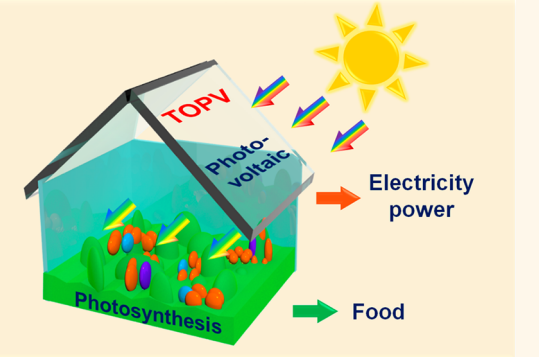

KEYWORDS: *infrared light, transparent, flexible, organic photovoltaic, photosynthesis*

Infrared (IR)-absorbing organic semiconductors are promising materials in semiconductor technology. One of the crucial reasons for this is that their absorption area of IR light is significant to optoelectronic devices.[1−7] In particular, compared with the traditional materials possessing a broad-band absorption area, the absorption of IR-absorbing organic semiconductors could be localized in a narrow IR light region by optimizing their chemical structure.[8−17] In other words, most visible light can be transmitted from these materials.

The absorption spectrum for photosynthesis is usually located within the region of 400−700 nm that is out of the primary absorption area of IR-absorbing organic semiconductors.[18] In a common greenhouse, a small degree of transparency of sunlight is sufficient for a large degree of plant growth. For instance, just a 10% transparency of visible light is enough for the growth of special organisms.[19] Within the energy distribution of the solar spectrum (the AM 1.5 G standard), 47% of the energy is occupied by the visible region, and the remaining 2% and 51% are, respectively, distributed in the ultraviolet and the IR regions, which means that the IR region has great potential with regard to power supplies.[20] In the field of optoelectronics, the simple and low-cost organic photovoltaics (OPVs) have demonstrated an alternative solution in energy conversion.[21−27] Hence, visible-light-trans-

Received: November 9, 2018
Accepted: January 2, 2019
Published: January 3, 2019

DOI: 10.1021/acsnano.8b08577
ACS Nano XXXX, XXX, XXX–XXX

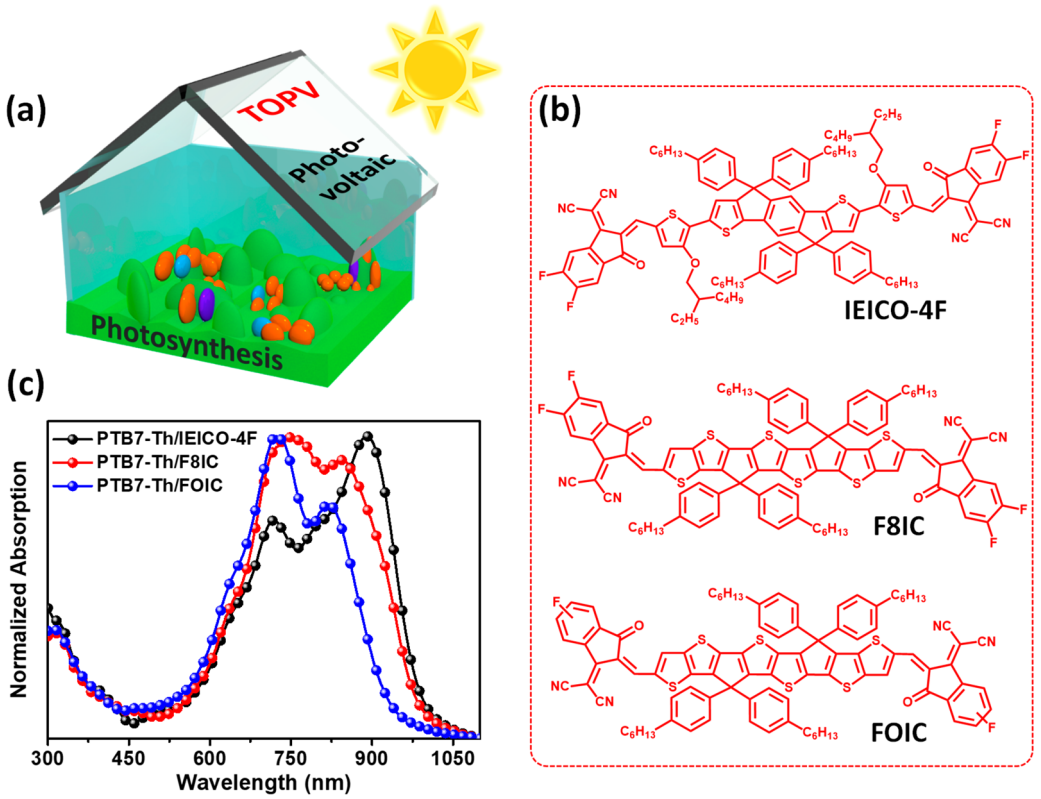

Figure 1. (a) Installation of flexible TOPVs on a greenhouse. (b) Chemical structure of IEICO-4F, F8IC, and FOIC. (c) Absorption spectra of different donor/acceptor blend films.

parent IR-absorbing organic semiconductors used for transparent OPV (TOPV) devices are promising in the distributed installment of roofs or windows.[28−38]

Here, flexible TOPV devices fabricated using different IR-absorbing organic semiconductors (IEICO-4F,[8] F8IC,[9] and FOIC)[10] were presented in which the IR-region sunlight was selectively absorbed for power generation and the visible sunlight penetrated the TOPV followed by absorption of plants for photosynthesis. Power-conversion efficiency (PCE) values of 10.02%, 8.92%, and 9.26% were achieved for the flexible TOPV devices based on different materials of IEICO-4F, F8IC, and FOIC, respectively. Meanwhile, average visible transmittance (AVT) values over 30% were acquired for these flexible TOPVs. Furthermore, plants showed a comparable growing tendency under the TOPV devices, which proved to be a feasible application of TOPV beyond photovoltaic.

RESULTS AND DISCUSSION

The schematic showing that TOPVs selectively absorbed the IR-region sunlight for power generation and that the penetrated visible sunlight was absorbed by plants for photosynthesis is shown in Figure 1a. The absorption region of active layers should meet the requirements for photovoltaics and photosynthesis simultaneously. IEICO-4F, F8IC, and FOIC (Figure 1b) were utilized as acceptors mixed with a polymer of PTB7-Th[39] (Figure S1) as a donor. The reason is that their blending film exhibited an outstanding spectrum-selective property of strong absorption in the IR area and favorable transmittance in the photosynthetic region (Figure 1c). In addition, the blending film is conformable with flexible substrates, which is more suitable for the complex application.

The transmittance and resistance of flexible substrates is important to the performance of TOPVs. The flexible TOPV was fabricated on polyethylene terephthalate (PET) substrates with silver (Ag) mesh as the electrode.[40] To further improve the conductivity of the substrate, a conductive polymer of poly(3,4-ethylenedioxythiophene)/poly(styrenesulfonate) (PEDOT:PSS, PH 1000) was spin-coated onto the Ag mesh, and a composite flexible substrate with a sheet resistance of ∼5 Ω/sq was acquired. A total of three blending films were deposited onto the composite substrate as active layers. The structure of flexible TOPV is PET/Ag mesh/PH 1000/zinc oxide (ZnO)/active layer/molybdenum oxide (MoO_3)/gold (Au)/Ag, as shown in Figure 2a. After the sunlight illuminated onto the PET side, the IR light was absorbed by the flexible TOPVs, and the visible light penetrated out from the ultrathin Ag film. In addition, the band energy diagram is displayed in Figure 2b. ZnO and MoO_3 worked as electron and hole transporting layers, respectively. Thin Au/Ag was used as the back transparent electrode.

All of the flexible TOPVs showed attractive photovoltaic properties, as shown in the current density−voltage (J−V) curves in Figure 2c, and the detailed data are summarized in Table 1. When PTB7-Th/IEICO-4F was used as an active layer, the flexible TOPV device yielded an average PCE of 9.66 ± 0.25% with an average short-circuit current density (J_{SC}) of 20.27 ± 0.20 mA/cm^2, an average open-circuit voltage (V_{OC}) of 0.707 ± 0.009 V, and an average fill factor (FF) of 67.4 ± 1.00%. If PTB7-Th/F8IC acted as an active layer, an average J_{SC} of 18.97 ± 0.38 mA/cm^2, an average V_{OC} of 0.687 ± 0.010 V, an FF of 66.7 ± 0.59%, and an average PCE of 8.69 ± 0.22% were achieved. A J_{SC} of 17.82 ± 0.67 mA/cm^2, a V_{OC} of 0.756 ± 0.006 V, an FF of 65.2 ± 0.36%, and an average PCE of 8.86

DOI: 10.1021/acsnano.8b08577
ACS Nano XXXX, XXX, XXX−XXX

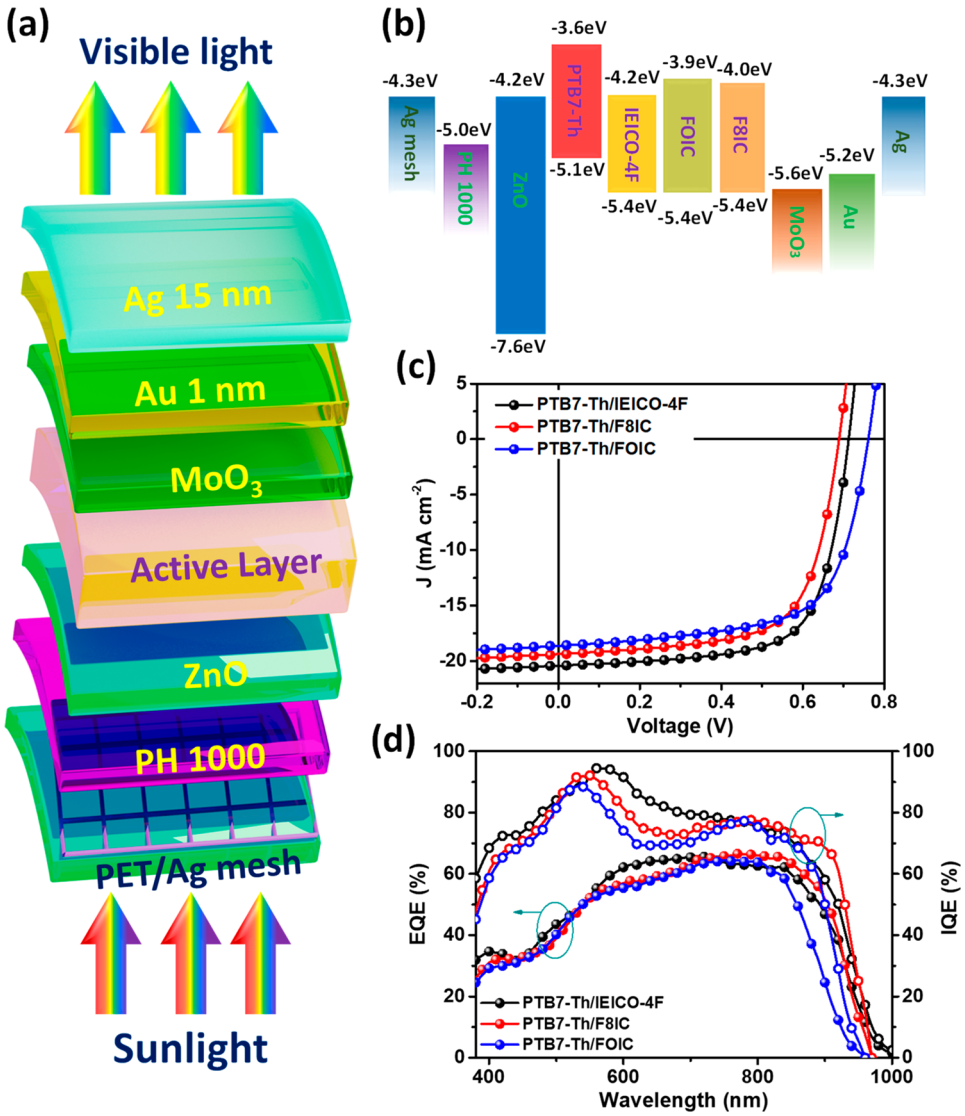

Figure 2. (a) Flexible TOPV structure of PET/Ag mesh/PH 1000/ZnO/active layer/MoO_3/Au (1 nm)/Ag (15 nm). Ag mesh/PH 1000 was used as the cathode, and a thin Au/Ag layer was used as the anode. (b) Band-energy diagram of materials used in the flexible TOPV. (c, d) *J*−*V* curves, EQE, and IQE spectra of flexible TOPV based on different IR-absorbing organic semiconductors. IQE spectra were calculated from EQE, reflection, and transmittance curves (Figure S4).

Table 1. Performances of TOPVs Based on Different IR-Absorbing Organic Semiconductors[a]

active layer	V_{OC} (V)	J_{SC} (mA/cm^2)	FF (%)	PCE (%)	best PCE (%)	AVT (%)
PTB7-Th:IEICO-4F	0.707 ± 0.009	20.27 ± 0.20	67.4 ± 1.00	9.66 ± 0.25	10.03	34.2
PTB7-Th:FOIC	0.756 ± 0.006	17.82 ± 0.67	65.2 ± 0.36	8.86 ± 0.32	9.26	31.0
PTB7-Th:F8IC	0.687 ± 0.010	18.97 ± 0.38	66.7 ± 0.59	8.69 ± 0.22	8.92	34.3

[a]Average values are calculated from five devices.

± 0.32% were acquired from a PTB7-Th/FOIC-based one. According to Figure S2, showing the photovoltaic properties of TOPV under bending conditions, the PCE of devices under a 60° bending angle only had a decrease of 10% compared to the PCE of the device without bending. Additionally, the external quantum efficiency (EQE) and internal quantum efficiency (IQE) spectra are shown in Figure 2d. The IQE value of the PTB7-Th/IEICO-4F-based solar cell is over 90% at 560 nm and the average IQE value is 81% in the range of 380−760 nm. The PTB7-Th/F8IC and PTB7-Th/FOIC also achieved the average IQE value over 70% in this region. This impressive IQE value indicated a high utilization of incident photons in the visible light region. According to the EQE spectra, the photoresponse region was mainly within the IR region, which was favorable for a higher transmittance in the visible area. Hence, the flexible TOPV could achieve a high PCE under visible-light-transparent conditions. Meanwhile, the calculated values of J_{SC} from the EQE spectra (Figure S3) lined up well with the J_{SC} values extracted from the *J*−*V* measurements. The simple fabrication process and various types of low-cost IR absorbing organic semiconductors present varied choices for general application.

Figure 3a is an optical photograph of a demo (6 cm × 6 cm) with a structure of PET/Ag mesh/PH 1000/ZnO/active layer/

DOI: 10.1021/acsnano.8b08577
ACS Nano XXXX, XXX, XXX−XXX

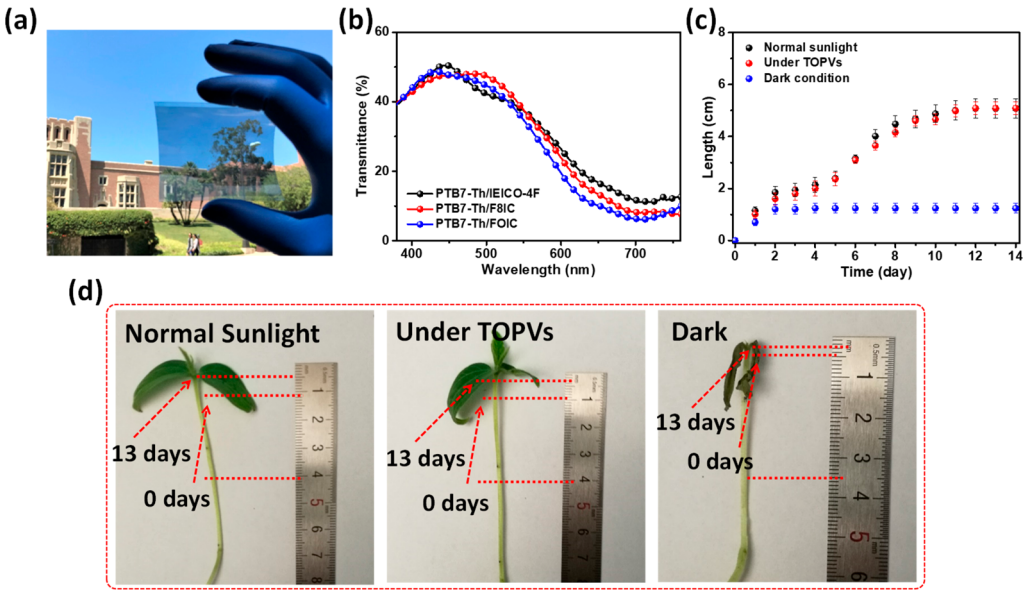

Figure 3. (a) Optical photograph of a demo (PET/Ag mesh/PH 1000/ZnO/active layer/MoO_3/Au/Ag) with a size of 6 cm × 6 cm. (b) Transmittance curves of flexible TOPV in the visible region. (c) Growing statuses of the mungs in different conditions. (d) Optical photographs of the length change of mungs after 13 days (the original length was 3 cm).

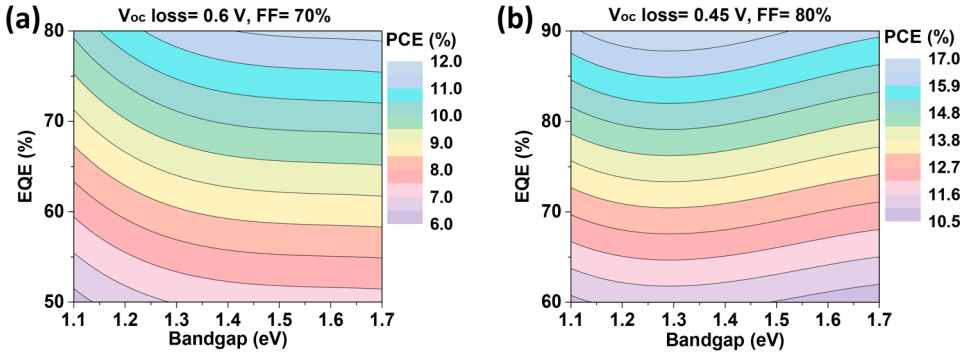

Figure 4. (a) Simulation PCE with an assumed average EQE value (IR region), FF, and V_{OC} loss of 70%, 0.7, and 0.6 V, respectively. (b) Simulation PCE with an assumed average EQE value (IR region), FF, and V_{OC} loss of 80%, 0.8, and 0.45 V, respectively.

MoO3/Au/Ag that is same as the small area TOPV under bending conditions. The back scenery could be clearly observed. The AVT values were 34.2%, 34.3%, and 31.4% for PTB7-Th/IEICO-4F, PTB7-Th/F8IC, and PTB7-Th/FOIC-based TOPVs, respectively, calculated from the following equation:

$$\mathrm{AVT} = \frac{\int T(\lambda)P(\lambda)S(\lambda)d(\lambda)}{\int P(\lambda)S(\lambda)\mathrm{d}(\lambda)}$$

where T is the transmission (Figure 3b), λ is the wavelength, P was the photonic response (Figure S5a), and S was the solar photon flux (Figure S5b, AM 1.5G).[29]

Mung beans (or "mungs") were chosen as the plant with which to observe the growing conditions. A PTB7-Th/IEICO-4F-based flexible TOPV was chosen as the photovoltaic power source, in which the penetrated visible light will be utilized for the photosynthesis of plants. Referential samples were mungs under normal sunlight or dark conditions. Figure 3c displayed the growing conditions of the mungs. Although the growing speed of the mungs under the TOPVs was slightly slower than when in normal sunlight, the final lengths demonstrated that their statuses were comparatively similar under the TOPVs or normal sunlight after 13 days. However, the samples under dark conditions were poor because of a lack of sunlight. As shown in Figure 3d, mungs under the TOPVs grew favorably compared with ones under normal sunlight after 13 days. However, the mungs without light wilted.

A summary of PCE and AVT of the best published results is demonstrated in Figure S6. This work is one of the highest performance devices. Meanwhile, the donors (PBDB-T and PDTP-DFBT) with different absorption spectra are chosen as active layers in TOPVs. As shown in Figure S7a, these materials have different film absorption spectra because of their different band gaps. To balance photovoltaics and photosynthesis, the TOPVs need a high PCE and low absorption in the visible region. The PBDB-T has much more absorption in visible light, which is not favorable for photosynthesis, and the devices based on PBDB-T have lower absorption than the PTB7-Th-based ones, as shown in Figure S7b. The PDTP-DFBT has a desired absorption region; however, the PCE is much lower. This is due to the unmatched energy level between PDTP-DFBT and IEICO-4F.

To further testify the potential of the IR-absorbing organic semiconductor based TOPV, a simulation of photovoltaic performance was conducted with a visible transmittance of

DOI: 10.1021/acsnano.8b08577
ACS Nano XXXX, XXX, XXX−XXX

30%.[1,41] Because the band gap of the IR-absorbing materials could be tuned, correspondingly, the absorption region of the TOPV could be tuned. Thus, we first depicted a PCE simulation based on current results. With an average EQE of 80% in the IR region (Figure S8a), the PCE of the TOPV was close to 12% with an assumed FF of 0.70 and *Voc* loss of 0.6 V (Figure 4a). Furthermore, a higher PCE of near 17% was obtained as shown in the simulated graph of Figure 4b, in which the assumed values of FF, *Voc* loss, and average EQE in the IR region (Figure S8b) were 0.8, 0.45 V, and 90%, respectively.

CONCLUSIONS

In summary, we presented the concept of "tailoring" sunlight for photovoltaic by TOPVs that were fabricated by IR-absorbing organic materials without influencing the transmittance of the visible light to plants growth. Owing to the outstanding absorption property within the IR region and transmittance in the visible area, the flexible TOPV not only achieved favorable electricity power generation but also ensured enough transmitted sunlight for the growth of plants. Our work demonstrated the great potential of TOPVs beyond simple photovoltaic applications.

EXPERIMENTAL SECTION

Materials. Flexible PET/Ag mesh/PEDOT:PSS substrate,[40] ZnO nanoparticle solution,[42] FOIC,[10] and F8IC[9] were prepared according to their respective previous publications. PTB7-Th and IEICO-4F were purchased from Cal-OS and Solarmer, respectively. 1-Chloronaphthalene (CN) was purchased from TCI. 1,8-Diiodooctane (DIO), chloroform (CF), chlorobenzene (CB), MoO_3, and Ag and were purchased from Sigma-Aldrich. Au was purchased from ESPI.

TOPV Fabrication. A 50 μm PET substrate was covered by a 100 μm hardening treatment PET to prevent distortion and keep surface cleaning of the PET substrate during device fabrication. A patterned nickel mold with a diagonal length of 90 μm, a width of 3 μm, and a height of 2 μm was prepared through electroforming. Afterward, a 7 μm ultraviolet resin is coated onto PET substrate by a nanoimprinting machine, followed by the patterning by the nickel mold under ultraviolet irradiation. The patterned groove was filled with silver ink, and the excess silver ink was removed by scraping. The substrate was sintered at 80 °C for 10 min. PEDOT:PSS (PH 1000) was spin-coated on the surface of PET/Ag mesh substrate at 2000 rpm for 1 min and then annealed at 100 °C for 15 min. ZnO nanoparticle solution (10 mg/mL) was spin-coated onto the prepared PET/Ag mesh/PEDOT:PSS substrate followed by annealing at 125 °C for 15 min. PTB7-Th/IEICO-4F was dissolved in CB solution (10 mg PTB7-Th and 15 mg IEICO-4F dissolved in 1 mL of CB with 30 μL CN) with stirring overnight at 60 °C, and PTB7-Th/F8IC (or FOIC) was dissolved in CF solution (6 mg PTB7-Th and 9 mg F8IC or FOIC dissolved in 1 mL of CF with 10 μL DIO) with stirring 30 min at 60 °C. Then, these solutions were spin-coated onto the ZnO layer. After that, 10 nm MoO_3, 1 nm Au, and 15 nm Ag were, respectively, evaporated onto the active layer under high-vacuum conditions (10^{-5} Pa). The active area of the solar cell was 0.1 cm^2.

Characterization. The transmittance and reflection of the TOPV and absorption of the active layers were measured by a 4100 Hitachi spectrofluorophotometer. The sheet resistance of the substrate (PET/Ag mesh/PH 1000) was conducted by a four-probe method. *J*–*V* performances of the solar cells were characterized under a simulated AM 1.5G spectrum (100 mW/cm^2) generated by an Oriel 9600 solar simulator. EQE curves were recorded by an Enlitech integrated system with a lock-in amplifier system. The length variations of mungs under different light condition were measured daily (six samples for different condition).

ASSOCIATED CONTENT

Supporting Information

The Supporting Information is available free of charge on the ACS Publications website at DOI: 10.1021/acsnano.8b08577.

Chemical structure of PTB7-Th, photovoltaic properties of TOPV under bending conditions, calculated J_{SC} from the EQE spectra, reflection and transmittance curves, curves of photonic response and solar photon flux (AM 1.5G), a summary of PCE and AVT of the published results, absorption curves of different band gap donors, *J*–*V* curves of TOPVs based on different active layers, and a simulation of the EQE spectra (PDF)

AUTHOR INFORMATION

Corresponding Authors

*E-mail: chengpei1989011@ucla.edu.
*E-mail: bqsun@suda.edu.cn.
*E-mail: yangy@ucla.edu.

ORCID

Yuqiang Liu: 0000-0003-3494-6390
Yaowen Li: 0000-0001-7229-582X
Kung-Hwa Wei: 0000-0002-0248-4091
Xiaowei Zhan: 0000-0002-1006-3342
Baoquan Sun: 0000-0002-4507-4578
Yang Yang: 0000-0001-8833-7641

Author Contributions

Y.L. and P.C. contributed equally to this work. Y.L. and P.C. designed and finished the experiment. T.L. synthesized the FOIC and F8IC. Y.L. presented the flexible substrate. R.W., S.C., Y.Z., and H.C optimized the active layer. Y.L., P.C., X.Z., B.S., and Y.Y. prepared the manuscript. B.S. and Y.Y. supervised the project. All authors discussed the results of the manuscript.

Notes

The authors declare no competing financial interest.

ACKNOWLEDGMENTS

Y.Y. acknowledges the Air Force Office of Scientific Research (AFOSR) (grant no. FA2386-18-1-4094), the Office of Naval Research (ONR) (grant no. N00014-17-1-2,484), and the UC Solar Program (grant no. MRPI 328368) for their financial support. X.Z. acknowledges the National Natural Science Foundation of China (grant no. 21734001) for financial support. Y.L. and B.S. acknowledge the National Key Research and Development Program of China (grant no. 2016YFA0202402), the National Natural Science Foundation of China (grant nos. 61674108 and 11811520119) for financial support, and the 111 Program and Collaborative Innovation Center of Suzhou Nano Science and Technology. K.W. acknowledges the Featured Areas Research Center Program, the Ministry of Science and Technology (grant no. M MOST 106-2221-E-009-132-MY3). Y.L. acknowledges the Chinese Scholars Council (grant no. 201706920073) for financial support. The authors also thank Shaun Tan for his insights on the manuscript.

REFERENCES

(1) Cheng, P.; Li, G.; Zhan, X.; Yang, Y. Next-Generation Organic Photovoltaics Based on Non-Fullerene Acceptors. *Nat. Photonics* **2018**, *12*, 131–142.

DOI: 10.1021/acsnano.8b08577
ACS Nano XXXX, XXX, XXX–XXX

(2) Hou, J.; Inganas, O.; Friend, R. H.; Gao, F. Organic Solar Cells Based on Non-Fullerene Acceptors. *Nat. Mater.* **2018**, *17*, 119−128.
(3) Zhang, J. Q.; Tan, H. S.; Guo, X. G.; Facchetti, A.; Yan, H. Material Insights and Challenges for Non-Fullerene Organic Solar Cells Based on Small Molecular Acceptors. *Nat. Energy* **2018**, *3*, 720−731.
(4) Li, Y. Molecular Design of Photovoltaic Materials for Polymer Solar Cells: toward Suitable Electronic Energy Levels and Broad Absorption. *Acc. Chem. Res.* **2012**, *45*, 723−733.
(5) Yan, C.; Barlow, S.; Wang, Z.; Yan, H.; Jen, A. K. Y.; Marder, S. R.; Zhan, X. Non-Fullerene Acceptors for Organic Solar Cells. *Nat. Rev. Mater.* **2018**, *3*, 18003.
(6) Liang, Y.; Yu, L. A New Class of Semiconducting Polymers for Bulk Heterojunction Solar Cells with Exceptionally High Performance. *Acc. Chem. Res.* **2010**, *43*, 1227−1236.
(7) Li, X.; Huang, H.; Bin, H.; Peng, Z.; Zhu, C.; Xue, L.; Zhang, Z.-G.; Zhang, Z.; Ade, H.; Li, Y. Synthesis and Photovoltaic Properties of a Series of Narrow Bandgap Organic Semiconductor Acceptors with Their Absorption Edge Reaching 900 nm. *Chem. Mater.* **2017**, *29*, 10130−10138.
(8) Yao, H.; Cui, Y.; Yu, R.; Gao, B.; Zhang, H.; Hou, J. Design, Synthesis, and Photovoltaic Characterization of a Small Molecular Acceptor with an Ultra-Narrow Band Gap. *Angew. Chem., Int. Ed.* **2017**, *56*, 3045−3049.
(9) Dai, S.; Li, T.; Wang, W.; Xiao, Y.; Lau, T. K.; Li, Z.; Liu, K.; Lu, X.; Zhan, X. Enhancing the Performance of Polymer Solar Cells *via* Core Engineering of NIR-Absorbing Electron Acceptors. *Adv. Mater.* **2018**, *30*, 1706571.
(10) Li, T.; Dai, S.; Ke, Z.; Yang, L.; Wang, J.; Yan, C.; Ma, W.; Zhan, X. Fused Tris(Thienothiophene)-Based Electron Acceptor with Strong Near-Infrared Absorption for High-Performance as-Cast Solar Cells. *Adv. Mater.* **2018**, *30*, 1705969.
(11) Li, Y.; Lin, J. D.; Che, X.; Qu, Y.; Liu, F.; Liao, L. S.; Forrest, S. R. High Efficiency Near-Infrared and Semitransparent Non-Fullerene Acceptor Organic Photovoltaic Cells. *J. Am. Chem. Soc.* **2017**, *139*, 17114−17119.
(12) Liu, F.; Zhou, Z.; Zhang, C.; Zhang, J.; Hu, Q.; Vergote, T.; Liu, F.; Russell, T. P.; Zhu, X. Efficient Semitransparent Solar Cells with High NIR Responsiveness Enabled by a Small-Bandgap Electron Acceptor. *Adv. Mater.* **2017**, *29*, 1606574.
(13) Chen, C.-C.; Dou, L.; Zhu, R.; Chung, C.-H.; Song, T.-B.; Zheng, Y. B.; Hawks, S.; Li, G.; Weiss, P. S.; Yang, Y. Visibly Transparent Polymer Solar Cells Produced by Solution Processing. *ACS Nano* **2012**, *6*, 7185−7190.
(14) Qin, H.; Li, L.; Guo, F.; Su, S.; Peng, J.; Cao, Y.; Peng, X. Solution-Processed Bulk Heterojunction Solar Cells Based on a Porphyrin Small Molecule with 7% Power Conversion Efficiency. *Energy Environ. Sci.* **2014**, *7*, 1397−1401.
(15) Li, W.; Hendriks, K. H.; Furlan, A.; Wienk, M. M.; Janssen, R. A. High Quantum Efficiencies in Polymer Solar Cells at Energy Losses Below 0.6 ev. *J. Am. Chem. Soc.* **2015**, *137*, 2231−2234.
(16) Campos, L. M.; Tontcheva, A.; Günes, S.; Sonmez, G.; Neugebauer, H.; Sariciftci, N. S.; Wudl, F. Extended Photocurrent Spectrum of a Low Band Gap Polymer in a Bulk Heterojunction Solar Cell. *Chem. Mater.* **2005**, *17*, 4031−4033.
(17) Wang, J.; Zhang, J.; Xiao, Y.; Xiao, T.; Zhu, R.; Yan, C.; Fu, Y.; Lu, G.; Lu, X.; Marder, S. R.; Zhan, X. Effect of Isomerization on High-Performance Nonfullerene Electron Acceptors. *J. Am. Chem. Soc.* **2018**, *140*, 9140−9147.
(18) Singhal, G.; Renger, G.; Sopory, S.; Irrgang, K. *Concepts in Photobiology: Photosynthesis and Photomorphogenesis*. Springer Science & Business Media: New York, 2012.
(19) Yang, Y.; Li, G. Transparent Organic Solar Cells for Agronomic Applications. U.S. Patent US2016/0013433A1, 2016, 1/14/2016, https://patents.google.com/patent/US20160013433A1/en.
(20) Lunt, R. R. Theoretical Limits for Visibly Transparent Photovoltaics. *Appl. Phys. Lett.* **2012**, *101*, No. 043902.
(21) Van Franeker, J. J.; Turbiez, M.; Li, W.; Wienk, M. M.; Janssen, R. A. A Real-Time Study of the Benefits of Co-Solvents in Polymer Solar Cell Processing. *Nat. Commun.* **2015**, *6*, 6229.
(22) Lipomi, D. J.; Tee, B. C.; Vosgueritchian, M.; Bao, Z. Stretchable Organic Solar Cells. *Adv. Mater.* **2011**, *23*, 1771−1775.
(23) Jinno, H.; Fukuda, K.; Xu, X.; Park, S.; Suzuki, Y.; Koizumi, M.; Yokota, T.; Osaka, I.; Takimiya, K.; Someya, T. Stretchable and Waterproof Elastomer-Coated Organic Photovoltaics for Washable Electronic Textile Applications. *Nat. Energy* **2017**, *2*, 780−785.
(24) Krebs, F. C. Fabrication and Processing of Polymer Solar Cells: A Review of Printing and Coating Techniques. *Sol. Energy Mater. Sol. Cells* **2009**, *93*, 394−412.
(25) Andersen, T. R.; Dam, H. F.; Hösel, M.; Helgesen, M.; Carlé, J. E.; Larsen-Olsen, T. T.; Gevorgyan, S. A.; Andreasen, J. W.; Adams, J.; Li, N.; Machui, F.; Spyropoulos, G. D.; Ameri, T.; Lemaître, N.; Legros, M.; Scheel, A.; Gaiser, D.; Kreul, K.; Berny, S.; Lozman, O. R.; et al.et al Scalable, Ambient Atmosphere Roll-to-Roll Manufacture of Encapsulated Large Area, Flexible Organic Tandem Solar Cell Modules. *Energy Environ. Sci.* **2014**, *7*, 2925.
(26) Brabec, C. J.; Heeney, M.; McCulloch, I.; Nelson, J. Influence of Blend Microstructure on Bulk Heterojunction Organic Photovoltaic Performance. *Chem. Soc. Rev.* **2011**, *40*, 1185−1199.
(27) Che, X. Z.; Li, Y. X.; Qu, Y.; Forrest, S. R. High Fabrication Yield Organic Tandem Photovoltaics Combining Vacuum- and Solution-Processed Subcells with 15% Efficiency. *Nat. Energy* **2018**, *3*, 422−427.
(28) Strohm, S.; Machui, F.; Langner, S.; Kubis, P.; Gasparini, N.; Salvador, M.; McCulloch, I.; Egelhaaf, H. J.; Brabec, C. J. P3HT: Non-Fullerene Acceptor Based Large Area, Semi-Transparent PV Modules with Power Conversion Efficiencies of 5%, Processed by Industrially Scalable Methods. *Energy Environ. Sci.* **2018**, *11*, 2225−2234.
(29) Traverse, C. J.; Pandey, R.; Barr, M. C.; Lunt, R. R. Emergence of Highly Transparent Photovoltaics for Distributed Applications. *Nat. Energy* **2017**, *2*, 849−860.
(30) Chang, S.-Y.; Cheng, P.; Li, G.; Yang, Y. Transparent Polymer Photovoltaics for Solar Energy Harvesting and Beyond. *Joule* **2018**, *2*, 1039−1054.
(31) Betancur, R.; Romero-Gomez, P.; Martinez-Otero, A.; Elias, X.; Maymó, M.; Martorell, J. Transparent Polymer Solar Cells Employing a Layered Light-Trapping Architecture. *Nat. Photonics* **2013**, *7*, 995−1000.
(32) Yu, W.; Jia, X.; Yao, M.; Zhu, L.; Long, Y.; Shen, L. Semitransparent Polymer Solar Cells with Simultaneously Improved Efficiency and Color Rendering Index. *Phys. Chem. Chem. Phys.* **2015**, *17*, 23732−23740.
(33) Shen, P.; Long, Y.; Wang, G.; Wang, Y.; Guo, W.; Shen, L. Semi-Transparent Polymer Solar Cells with Optical Adjusting Layers. *J. Mater. Chem. C* **2018**, *6*, 9494−9500.
(34) Shen, P.; Wang, G.; Kang, B.; Guo, W.; Shen, L. High-Efficiency and High-Color-Rendering-Index Semitransparent Polymer Solar Cells Induced by Photonic Crystals and Surface Plasmon Resonance. *ACS Appl. Mater. Interfaces* **2018**, *10*, 6513−6520.
(35) Cui, Y.; Yang, C.; Yao, H.; Zhu, J.; Wang, Y.; Jia, G.; Gao, F.; Hou, J. Efficient Semitransparent Organic Solar Cells with Tunable Color Enabled by an Ultralow-Bandgap Nonfullerene Acceptor. *Adv. Mater.* **2017**, *29*, 1703080.
(36) Xu, G.; Shen, L.; Cui, C.; Wen, S.; Xue, R.; Chen, W.; Chen, H.; Zhang, J.; Li, H.; Li, Y.; Li, Y. High-Performance Colorful Semitransparent Polymer Solar Cells with Ultrathin Hybrid-Metal Electrodes and Fine-Tuned Dielectric Mirrors. *Adv. Funct. Mater.* **2017**, *27*, 1605908.
(37) Jeon, I.; Delacou, C.; Kaskela, A.; Kauppinen, E. I.; Maruyama, S.; Matsuo, Y. Metal-Electrode-Free Window-Like Organic Solar Cells with P-Doped Carbon Nanotube Thin-Film Electrodes. *Sci. Rep.* **2016**, *6*, 31348.
(38) Emmott, C. J. M.; Röhr, J. A.; Campoy-Quiles, M.; Kirchartz, T.; Urbina, A.; Ekins-Daukes, N. J.; Nelson, J. Organic Photovoltaic

DOI: 10.1021/acsnano.8b08577
ACS Nano XXXX, XXX, XXX−XXX

Greenhouses: A Unique Application for Semi-Transparent PV? *Energy Environ. Sci.* **2015**, *8*, 1317−1328.
(39) Liao, S. H.; Jhuo, H. J.; Cheng, Y. S.; Chen, S. A. Fullerene Derivative-Doped Zinc Oxide Nanofilm as the Cathode of Inverted Polymer Solar Cells with Low-Bandgap Polymer (PTB7-Th) for High Performance. *Adv. Mater.* **2013**, *25*, 4766−4771.
(40) Li, Y.; Meng, L.; Yang, Y. M.; Xu, G.; Hong, Z.; Chen, Q.; You, J.; Li, G.; Yang, Y.; Li, Y. High-Efficiency Robust Perovskite Solar Cells on Ultrathin Flexible Substrates. *Nat. Commun.* **2016**, *7*, 10214.
(41) Dennler, G.; Scharber, M. C.; Ameri, T.; Denk, P.; Forberich, K.; Waldauf, C.; Brabec, C. J. Design Rules for Donors in Bulk-Heterojunction Tandem Solar Cells-Towards 15% Energy-Conversion Efficiency. *Adv. Mater.* **2008**, *20*, 579−583.
(42) Sun, B.; Sirringhaus, H. Solution-Processed Zinc Oxide Field-Effect Transistors Based on Self-Assembly of Colloidal Nanorods. *Nano Lett.* **2005**, *5*, 2408−2413.

DOI: 10.1021/acsnano.8b08577
ACS Nano XXXX, XXX, XXX−XXX